Analysis of the wave properties of a new two-lane continuum model with the coupling effect

2012 Chinese Phys. B 21 015201

(http://iopscience.iop.org/1674-1056/21/1/015201)

Analysis of the wave properties of a new two-lane continuum model with the coupling effect

Arvind Kumar Gupta[a)†] and Sapna Sharma[b)]

[a)] *Department of Mathematics, Indian Institute of Technology Ropar, Punjab* 140001, *India*

[b)] *Department of Mathematics, Birla Institute of Technology & Science Pilani, Rajasthan* 333031, *India*

(Received 22 June 2011; revised manuscript received 2 August 2011)

A multilane extension of the single-lane anisotropic continuum model (GK model) developed by Gupta and Katiyar for traffic flow is discussed with the consideration of the coupling effect between the vehicles of different lanes in the instantaneous traffic situation and the lane-changing effect. The conditions for securing the linear stability of the new model are presented. The shock and the rarefaction waves, the local cluster effect and the phase transition are investigated through simulation experiments with the new model and are found to be consistent with the diverse nonlinear dynamical phenomena observed in a real traffic flow. The analysis also focuses on empirically observed two-lane phenomena, such as lane usage inversion and the density dependence of the number of lane changes. It is shown that single-lane dynamics can be extended to multilane cases without changing the basic properties of the single-lane model. The results show that the new multilane model is capable of explaining some particular traffic phenomena and is in accordance with real traffic flow.

Keywords: two-lane traffic, numerical simulation, lane usage inversion

PACS: 52.35.Mw **DOI:** 10.1088/1674-1056/21/1/015201

1. Introduction

Mobility is nowadays one of the most important ingredients of a modern society, so the investigation of traffic flow has attracted the interest of physicists and engineers for more than half a century. Since the 1950s, various traffic flow models, including the microscopic car-following model, the cellular automata (CA) model, the macroscopic continuum model and the mesoscopic gas-kinetic model, have been proposed to study complex traffic phenomena. Most models focus on the traffic flow on a single lane highway. However, in real traffic, a highway usually has more than one lane. Therefore, developing a multilane traffic flow model that can deal with the interlane coupling between adjacent lanes and is consistent with the diverse nonlinear dynamical phenomena observed in freeway traffic has become an important topic in the field of traffic science.

Macroscopic traffic flow models, which concentrate on the collective behaviour of vehicles, have played important roles in describing many nonlinear complexities. They are needed for understanding the collective behaviour of traffic in designing efficient control strategies, developing and controlling on-line speed-control systems, and evaluating the average travel time, fuel consumption, vehicle emissions, etc. Fundamentals of traffic flow modeling and control are the basic relationship between three traffic states: flow rate q, mean velocity v and vehicle density ρ. Since the seminal work by Lighthill and Whitham[1] on the kinetic theory of traffic flow, vehicles have often been considered as interacting particles, and traffic flow can be considered as a one-dimensional compressible flow of those particles. Due to analogies with gas theory[2] and fluid dynamics (Lighthill and Whitham,[1] Payne,[3] Kerner and Konhäuser,[4] Zhang,[5] Berg *et al.*[6]), modelling and simulating traffic flow increasingly attracts the attention of physicists and engineers. The study of continuum models began with the LWR model developed independently by Lighthill and Whitham,[1] and Richards.[7] The LWR model is known as a simple continuum model, in which the relationships among the three aggregate variables (ρ, v, and q) are modeled on a long homogeneous freeway. The LWR model employs the conservation equation in the following form:

$$\frac{\partial \rho}{\partial t} + \frac{\partial q}{\partial x} = s\,(x,t)\,. \tag{1}$$

Equation (1) is not a self-consistent model and needs

†Corresponding author. E-mail: akgupta@iitrpr.ac.in

an additional relation, which is supplemented by the equation of traffic flow

$$q = \rho v, \tag{2}$$

and a relationship between the mean velocity and the traffic density under a steady-state uniform flow

$$v = v_{\mathrm{e}}(\rho), \tag{3}$$

where $v_{\mathrm{e}}(\rho)$ is the equilibrium velocity; x and t represent the space and the time, respectively. If the freeway has no on-off ramp, then $s(x,t) = 0$; otherwise, $s(x,t) \neq 0$.

The waves described by the simple continuum model are kinematic waves in the sense that no dynamic law is used in the model. It is simple yet sufficiently powerful to describe the most basic traffic flow phenomena, such as the traffic congestion formation and the dissipation in a dense traffic.

However, the LWR model has its deficiencies. The most fatal one is that the speed is solely determined by the equilibrium speed density relationship. No fluctuation of speed around the equilibrium values is allowed. Thus, the model is not suitable for the description of non-equilibrium situations, such as the stop-and-go traffic and the forward propagation of disturbances in a heavy traffic.

In the past decades, many efforts were devoted to improving the LWR model through developing higher-order models, which use a dynamic equation or a momentum equation for the speed to replace the equilibrium relationship. In the momentum equation, the acceleration and the inertia of the driving are taken into account. Hence, the higher-order models overcome some of the deficiencies presented in the simple continuum model and improve their ability to reproduce complex traffic behaviours. Perhaps the most well known result of those efforts is the higher-order model developed by Payne.[3] In the Payne model, the fluctuation of speed around the equilibrium values is allowed, thus, the model is suitable for the description of non-equilibrium situations. Later, several authors (e.g., Kerner and Konhäuser,[4] Zhang[5]) suggested a considerable number of modifications to the Payne model. Berg *et al.*[6] proposed a continuum version of the car following OV model[8] by using a series expansion of the headway in terms of the density.

However, as pointed out by Daganzo,[9] the Payne model (and the other listed nonequilibrium models) has two families of characteristics, along which the traffic information is transmitted. One is slower and the other is faster than the speed of the traffic stream that carries them. The faster characteristic leads to a gas-like behaviour, as the vehicle from behind can force the vehicles in front to speed up[10] and the diffusion causes the 'wrong-way' travel.[9] One fundamental principal of the traffic flow is that vehicles are anisotropic and respond only to frontal stimuli. To overcome this difficulty, Aw and Rascle,[11] Jiang *et al.*,[12] and Zhang[13] proposed a second class of higher-order models. Aw and Rascle[11] developed a model to suppress the gas-like behaviour by replacing the space derivative of the density with a convective derivative. Both Jiang *et al.*[12] and Zhang[13] derived a macroscopic equation with anisotropy from car-following models. Those models are different from the first class of models in the sense that the anticipation term is a speed gradient term instead of a density gradient term. Thus, those models are referred to as the speed gradient (SG) models in traffic flow literature. Recently, Jiang and Wu[14] further analysed the structural properties of the solutions to the speed gradient traffic flow model. They showed that the characteristic speed of the model was not larger than the macroscopic flow speed. However, the propagation speed of the disturbance, c_0, in this model was a constant. In fact, the propagation speed of the disturbance in the Payne type model should depend on the density.[15,16] Subsequently, Xue and Dai[17] improved the model by taking c_0 as a function of the density, which indicates that the undesirable wrong-way travel phenomenon and the gas-like behaviour have been eliminated and the formation and the diffusion of the traffic shock can be better simulated in their model. Gupta and Katiyar[18] developed an improved anisotropic continuum model based on the car-following model given by Jiang *et al.*[12] and used the series expansion between the headway and the density given by Berg *et al.*[6] The qualitative properties, the shock waves and the jams were also investigated in their model.[19]

In all of the above models, the following vehicle is not allowed to overtake the leading vehicle. Hence, those models are not appropriate to describe the traffic flow on freeways with multiple lanes. Recently, multilane models have been developed in an attempt to explain some puzzling phenomena related to the lane-changing behaviour. Macroscopic traffic flow models are not so easily extended to a multilane system as compared to microscopic models. Daganzo[20] presented a continuum theory of traffic dynamics for freeways with special lanes. The LWR model is extended

to two lanes allocated for two sorts of vehicles (one for faster vehicles and the other for slower vehicles) and has the following form:

$$\frac{\partial \rho_m}{\partial t} + \frac{\partial q_m}{\partial x} = \boldsymbol{S}, \tag{4}$$

where $\boldsymbol{S} = (s_{12} - s_{21}, s_{21} - s_{12})^{\mathrm{T}}$, ρ_m and q_m are the traffic density and the flow rate on lane m ($m = 1, 2$), respectively, and s_{mn} represents the lane-changing rate from lane m to lane n. The speed and the density based on the density ratio of the two lanes were studied and the traffic flow model for each of the four ρ_1–ρ_2 regions were formulated by Daganzo.[20] Considering the special traffic conditions in Chinese cities (e.g. untidy flows and lower speeds on roads), Wu[21] proposed a multilane traffic model by equalizing all lane densities through averaging them, which conflicts with real traffic since the density on the lane allocated for faster vehicles is generally smaller than that on the lane allocated for slower vehicles. Tang and Huang[22] extended the speed gradient model to two-lane freeways, in which the momentum equation proposed by Jiang *et al.*[12] was integrated into Daganzo's modeling framework for multilane traffic flow[20] and the nonequilibrium phenomena such as stop-and-go waves were reproduced. Huang *et al.*[23] further extended the work of Tang and Huang[22,24] by allowing the vehicles on both lanes to change their lanes according to the traffic conditions. Tang *et al.*[25] also extended the speed gradient model for two lanes and discussed the lane usage inversion and the lane-changing frequency phenomena. Han *et al.*[26] developed a two-lane traffic flow model with the consideration of the coupling effect by embedding two delay time scales. Recently, Hua and Han[27] extended the viscous continuum model for a single lane to two-lane freeways by considering the coupling and the lane-changing effects of the vehicles on two adjacent lanes. Most of the above discussed models are either anisotropic or with a constant propagation speed of the disturbance c_0 independent of the density. However, Zhang[28] pointed out that the anisotropic property could not be expected to hold in the multilane traffic where vehicles were allowed to change their lanes.

In this paper, we attempt to make a multilane continuum model to describe the asymmetric two-lane traffic with the consideration of the coupling effect. In addition, the vehicles on both lanes are allowed to change their lanes according to the traffic conditions. This new model overcomes the problems of negative flows and negative speeds (i.e., wrong-way travel) that exist in almost every higher-order continuum model. However, it is not a fully anisotropic continuum model, as a traffic dependent anisotropic factor controls the isotropic character and the diffusive influence in special circumstances, and therefore it can describe the traffic-flow dynamics more realistically on two-lane freeways. We also investigate the lane change rate resulting in the shock wave and the local cluster effect in the two-lane freeway.

In the next section, we present an improved continuum model based on the car-following model and extend it to multilane traffic flow considering the coupling and the lane-changing effects of the vehicles on the adjacent lanes. Some qualitative properties including the stability analysis of the new multi-lane model are also discussed in next section. A numerical simulation is described in Section 3. We then analyse some nonequilibrium phenomena, such as shock waves and rarefaction waves, in Section 4 and the local cluster effect and the phase transition in Section 5. Finally, in Section 6, we provide a conclusion on our results.

2. Model and its mathematical properties

2.1. New continuum model

The car-following model is developed to model the motion of vehicles following each other on a single lane without overtaking. The car-following models present the only class of models that describe each vehicle in a deterministic manner including the response to local variables such as speed, headway and change of headway. Therefore they seem to be of great importance to autonomous cruise control systems, which should stabilize the flow and maximize the flow rate. In this paper, we follow Jiang's model[12] of road traffic, in which the acceleration of every vehicle is determined by

$$\frac{\mathrm{d}v_n(t)}{\mathrm{d}t} = \frac{1}{T}[V_{\mathrm{e}}(b_n) - v_n(t)] + \alpha\lambda\Delta v, \tag{5}$$

where $\Delta v = v_{n-1}(t) - v_n(t)$, with v_{n-1} and v_n being the speeds of the leading and the following cars, respectively, V_{e} is the optimal velocity function, b_n is the headway and T is the relaxation time, which corresponds to a driver's reaction time. It is generally believed that the headway can be written as a perturbation series.[6] Inserting the approximate expression

about the headway into Eq. (5), we can easily obtain the traffic flow dynamics equation.[18,19] The full description of this new non-equilibrium theory is given by a system of partial differential equations with the first being the vehicle conservation and the second the speed dynamics,

$$\rho_t + (\rho v)_x = 0, \tag{6}$$

$$\frac{\partial v}{\partial t} + v\frac{\partial v}{\partial x} = \frac{1}{T}[\bar{V}(\rho) - v] + \frac{\bar{V}'(\rho)}{T}\left[\frac{1}{2\rho}\frac{\partial \rho}{\partial x} + \frac{1}{6\rho^2}\frac{\partial^2 \rho}{\partial x^2} - \frac{1}{2\rho^3}\left(\frac{\partial \rho}{\partial x}\right)^2\right] - 2\beta c(\rho)\frac{\partial v}{\partial x}, \tag{7}$$

where $\bar{V}'(\rho) = \mathrm{d}\bar{V}(\rho)/\mathrm{d}\rho$, β is a non-negative dimensionless parameter, and $c(\rho) < 0$ is the traffic sound speed given by

$$c^2(\rho) = -\frac{\bar{V}'(\rho)}{2T}. \tag{8}$$

These two equations are analogous to the continuity and the Navier–Stokes equations, respectively. Here $\rho(x,t)$ is the local vehicle density, $v(x,t)$ is the local velocity and the traffic flow is understood as $q(x,t) = \rho(x,t)v(x,t)$. The $\bar{V}(\rho)$ is the safe velocity that is achieved in steady-state homogeneous traffic flow. The intrinsic properties on the main highway are prescribed by $\bar{V}(\rho)$ and two parameters T and $c(\rho)$. Driver's reaction time T is taken as a constant in our model, while $c(\rho)$ represents the anticipation parameter, which will vary with $\rho(x,t)$. In all previously developed models, the anticipation is taken as a constant, but in real situations, the anticipation parameters depends on the traffic density.[6,16,29]

2.2. Extended continuum model for two-lane traffic

In this section, we extend the new continuum model for two-lane freeways by considering lane change behaviour. To model this effect, a source term is added to the continuity equation to describe the flow rate changing from the other lane and a sink term is added to the continuity equation to describe the flow rate changing to the other lane. We also take the coupling effect into account for the interaction between vehicles on the two lanes. Accordingly, two terms are added in the speed dynamic equation. Each should satisfy the following law of conservation of vehicles:

$$\frac{\partial \rho_m}{\partial t} + \frac{\partial(\rho_m v_m)}{\partial x} = s_{nm} - s_{mn}. \tag{9}$$

It states that the density changes according to the balance between the inflow and the outflow of vehicles of lane m along a topographically homogeneous highway section without any on-off ramp. The velocity dynamics equation for lane m is given by

$$\frac{\partial v_m}{\partial t} + v_m\frac{\partial v_m}{\partial x} = \frac{1}{T_m}[\bar{V_m}(\rho_m, \gamma\rho_n) - v_m] + \frac{\bar{V_m}'(\rho_m, \gamma\rho_n)}{T_m} \times \left[\frac{1}{2\rho_m}\frac{\partial \rho_m}{\partial x} + \frac{1}{6\rho_m^2}\frac{\partial^2 \rho_m}{\partial x^2} - \frac{1}{2\rho_m^3}\left(\frac{\partial \rho_m}{\partial x}\right)^2\right] - 2\beta c_m(\rho_m)\frac{\partial v_m}{\partial x} + r_1 s_{mn} - r_2 s_{nm}, \tag{10}$$

where γ describes the coupling effect, which is taken as a constant based on the principle of the coupling interaction,[27] $m = 1, 2$ denotes the m-th lane, and $n = 1, 2$ $(m \neq n)$ denotes the other lane. The model given by Eqs. (9) and (10) for a specific lane, if the coupling effect and its lane-changing rate are not taken into account ($\gamma = 0$ and $S = 0$), is formally the same as the continuum model on a single lane proposed by Gupta and Katiyar.[18,19] According to Liu's idea[30] and Tang's model,[25] we suppose that the analogy terms of the lane-changing rate have the following forms:

$$s_{12} = aQ_{\mathrm{e}1}\rho_1\left[1 - \left(\frac{\rho_2}{\rho_{2,\mathrm{jam}}}\right)^{\sigma}\right], \tag{11}$$

$$s_{21} = a(1 + b(Q_{\mathrm{e}1} - Q_{\mathrm{e}2}))Q_{\mathrm{e}1}\rho_2 \times \left[1 - \left(\frac{\rho_1}{\rho_{1,\mathrm{jam}}}\right)^{\varphi}\right], \tag{12}$$

where a and b are constants, $\rho_{m,\mathrm{jam}}$ is the jam density of the m-th lane, $Q_{\mathrm{e}m}$ is the equilibrium flow, $Q_{\mathrm{e}m} = \rho V_{\mathrm{e}m}(\rho)$, and σ and φ are the parameters that reflect the intensity of the lane-changing effect from one lane to another $(0 \leq \sigma \leq \varphi \leq 1)$ and depend on the condition of the roads. For symmetric lane change rules, $Q_{\mathrm{e}1} = Q_{\mathrm{e}2}$, while $Q_{\mathrm{e}1} \neq Q_{\mathrm{e}2}$ corresponds to asymmetric lane change rules.

The above model for the lane-changing rate is suitable for the real traffic flow, as it maintains the physical properties of the traffic flow even under the extreme conditions. For example, the lane-changing rate s_{12} should be zero when $\rho_2 = \rho_{2,\mathrm{jam}}$ or $\rho_1 = 0$. Furthermore, it is easy to understand from Eqs. (11) and (12) that the lane-changing rate depends on the equilibrium speed density relationship of the present lane and on the coupling density of the other lane.

2.3. Propagation speeds

The system given by Eqs. (9) and (10) for a single lane has a similar structure to Berg *et al.*'s[6] and Zhou *et al.*'s models,[29] and is more general than those models. Our model has an additional term $2\beta\, c(\rho)\, v_x$. Moreover, the term $c(\rho)$ depends on the density and varies with the OV function. These differences, however, are not structural differences. So we would expect that the new model behaves roughly the same as Berg *et al.*'s and Zhou *et al.*'s models and perhaps gives a more accurate description of the traffic flow owing to its greater generality. Comparing our new model for two lanes with the recently developed model by Han *et al.*[26] and Tang *et al.*,[25] we can see that the new model is viscous and contains two new motion equations as compared to the continuum model presented by Daganzo.[20]

The system composed of Eqs. (9) and (10) can be expressed in the vector notation as

$$\frac{\partial \boldsymbol{V}}{\partial t} + \boldsymbol{A}\frac{\partial \boldsymbol{V}}{\partial x} = \boldsymbol{E}, \tag{13}$$

where $\boldsymbol{V} = \begin{bmatrix} \rho_1 \\ v_1 \\ \rho_2 \\ v_2 \end{bmatrix}$,

$$\boldsymbol{E} = \begin{bmatrix} s_{21} - s_{12} \\ \dfrac{1}{T_1}[\bar{V}_1 - v_1] + \dfrac{\bar{V}_1{}'}{T_1}\left[\dfrac{1}{6\rho_1^2}\dfrac{\partial^2\rho_1}{\partial x^2} - \dfrac{1}{2\rho_1^3}\left(\dfrac{\partial\rho_1}{\partial x}\right)^2\right] + r_1 s_{12} - r_2 s_{21} \\ s_{12} - s_{21} \\ \dfrac{1}{T_2}[\bar{V}_2 - v_2] + \dfrac{\bar{V}_2{}'}{T_2}\left[\dfrac{1}{6\rho_2^2}\dfrac{\partial^2\rho_2}{\partial x^2} - \dfrac{1}{2\rho_2^3}\left(\dfrac{\partial\rho_2}{\partial x}\right)^2\right] + r_1 s_{21} - r_2 s_{12} \end{bmatrix},$$

$$\boldsymbol{A} = \begin{bmatrix} v_1 & \rho_1 & 0 & 0 \\ -\dfrac{\bar{V}_1{}'}{2T_1\rho_1} & v_1 + 2\beta c_1 & 0 & 0 \\ 0 & 0 & v_1 & \rho_2 \\ 0 & 0 & -\dfrac{\bar{V}_2{}'}{2T_2\rho_2} & v_2 + 2\beta c_2 \end{bmatrix}.$$

It is straightforward to calculate eigenvalues λ of matrix $\boldsymbol{A}$ by setting

$$|\,\boldsymbol{A} - \lambda\boldsymbol{I}| = 0, \tag{14}$$

where $\boldsymbol{I}$ is the identity matrix. Thus, we have

$$\begin{aligned} \lambda_{11} &= v_1 + (\beta + \sqrt{1+\beta^2})\, c_1, \\ \lambda_{12} &= v_1 + (\beta - \sqrt{1+\beta^2})\, c_1, \\ \lambda_{21} &= v_2 + (\beta + \sqrt{1+\beta^2})\, c_2, \\ \lambda_{22} &= v_2 + (\beta - \sqrt{1+\beta^2})\, c_2. \end{aligned}$$

The system given by Eq. (13) has two families of traffic sound waves, shock and rarefaction waves, one family for each characteristic field on each lane. For the first characteristic field, the properties of these waves are quantitatively identical to those of the LWR model, because $\lambda_{11} \leq v_1$ and $\lambda_{21} \leq v_2$. For the second characteristic, the waves behave quite differently, as they travel faster than the traffic ($\lambda_{12} \geq v_1$ and $\lambda_{22} \geq v_2$). This means that the future conditions of the traffic flow will be affected by the traffic conditions behind the flow. Zhang[28] pointed out that the anisotropic property of the traffic could not be expected to hold in the multilane traffic because of the lane changing. Such type of behaviour, however, can be controlled by factor β in our model. We call it the anisotropic factor. Note that for $\beta \gg 1$, the second characteristic approaches the microscopic flow speed on each lane. Thus, the information can never reach vehicles from behind and the rear disturbances cannot propagate forward on each lane. However, for smaller values of β, it also guarantees that in a system consisting of two lanes, rear disturbances will affect the driving behaviour of the leading vehicles, because lane-changing is allowed in these two-lane traffic systems.

2.4. Stability analysis

In order to check whether the newly developed multilane model can describe the nonlinear theory of the cluster effect under a small perturbation in the traffic flow, i.e., the effect of the appearance of a region of high density and low average velocity vehicles in an initially homogeneous flow, we study the propagation stability conditions using the linear stability method in this section. It is difficult to obtain an analytical result about the stability of the two-lane traffic flow when lane-changing is allowed. According to the method introduced by Tang and Huang,[22] Huang *et al.*,[23] and Hua and Han,[27] the steady-state solution of the extended new model can be obtained by setting the derivative terms in Eqs. (9) and (10) to zero. Then we have

$$Q_{\rm e1}\rho_1\left[1-\left(\frac{\rho_2}{\rho_{2,\rm jam}}\right)^{\sigma}\right] = (1+b(Q_{\rm e1}-Q_{\rm e2}))Q_{\rm e1}\rho_2\left[1-\left(\frac{\rho_1}{\rho_{1,\rm jam}}\right)^{\varphi}\right], \quad (15)$$

$$\frac{1}{T_m}[\bar{V}_m(\rho_m,\gamma\rho_n)-v_m]+r_1 s_{mn}-r_2 s_{nm}=0. \quad (16)$$

We assume that ρ_m^0 and $v_m^0=\bar{V}_m(\rho_m^0,\gamma\rho_n^0)$ are the steady-state solutions of Eqs. (9) and (10). The analogous criterion for the continuum model may be found by linearizing the model around some initial values ρ_m^0 and v_m^0

$$\rho_m=\rho_m^0+\hat{\rho}_m(x,t), \quad (17)$$

$$v_m=v_m^0+\hat{v}_m(x,t), \quad (18)$$

where ρ_m and v_m are the perturbed solutions of Eqs. (9) and (10), with $\hat{\rho}_m(x,t)$ and $\hat{v}_m(x,t)$ being small perturbations to the steady-state solutions ρ_m^0 and v_m^0, respectively. After taking the Taylor series expansions of the perturbed equations at ρ_m^0 and v_m^0 and neglecting higher-order terms of $\hat{\rho}_m(x,t)$, $\hat{v}_m(x,t)$ and the coupling terms, we obtain the following linearized perturbation equations:

$$\frac{\partial\hat{\rho}_m}{\partial t}+\rho_m^0\frac{\partial\hat{v}_m}{\partial x}+v_m^0\frac{\partial\hat{\rho}_m}{\partial x}=0, \quad (19)$$

$$\frac{\partial\hat{v}_m}{\partial t}+v_m^0\frac{\partial\hat{v}_m}{\partial x}=\frac{[\bar{V}_m'(\rho_m^0,\gamma\rho_n^0)-\hat{v}_m]}{T_m}+\frac{\bar{V}_m'}{T_m}\left[\frac{1}{2\rho_m^0}\frac{\partial\hat{\rho}_m}{\partial x}+\frac{1}{6(\rho_m^0)^2}\frac{\partial^2\hat{\rho}_m}{\partial x^2}\right]-2\beta\, c_m^0\frac{\partial\hat{v}_m}{\partial x}, \quad (20)$$

where $c_m^0=c(\rho_m^0)$, $\bar{V}_m'=\bar{V}_m'(\rho_m^0,\gamma\rho_n^0)$, and $m=1,2$.

The linear stability of the system can be determined by examining the sinusoidal solution of the perturbed Eqs. (19) and (20). To determine the stability condition of system (13), we calculate the eigenvalue $\omega(k)$ of a harmonic disturbance

$$\bar{\boldsymbol{f}}(x,t)=\begin{pmatrix}\hat{\rho}_m(x,t)\\ \hat{v}_m(x,t)\end{pmatrix}=\begin{pmatrix}\hat{\rho}_m^0\\ \hat{v}_m^0\end{pmatrix}\exp\{\mathrm{i}\,[k\,x-\omega_m(k)\,t]\}. \quad (21)$$

Using Eq. (21), we can rewrite Eqs. (19) and (20) for the nontrivial solution as

$$\begin{vmatrix}\mathrm{i}(kv_m^0-\omega_m) & \mathrm{i}\,k\rho_m^0\\ -\dfrac{\bar{V}_m'}{T_m}-\dfrac{\mathrm{i}\,k\bar{V}_m'}{2T_m\rho_m^0}+\dfrac{\bar{V}_m'k^2}{6T_m(\rho_m^0)^2} & \mathrm{i}(kv_m^0-\omega_m)+\dfrac{1}{T_m}+2\beta\, c_m^0\,\mathrm{i}\,k\end{vmatrix}=0. \quad (22)$$

We obtain

$$\omega_m(k)=k(v_m^0+\beta c_m^0)-\frac{\mathrm{i}}{2T_m}\left[1\pm\sqrt{1+2T_m\bar{V}_m'\left(k^2(\beta^2+1)-\frac{\mathrm{i}\,\beta k}{T_m c_m^0}-2\,\mathrm{i}\,k\rho_m^0+\frac{\mathrm{i}\,k^3}{3\rho_m^0}\right)}\right]. \quad (23)$$

The traffic flow will remain stable as long as the imaginary part of ω_m is negative. We can obtain the neutral stability condition as

$$(\rho_m^0)^2-\frac{2\beta c_m^0\rho_m^0}{\bar{V}_m'}<-\left[\frac{(1+\beta^2)}{2T_m\bar{V}_m'}\right]. \quad (24)$$

This shows that the model is stable against all infinitesimal perturbations for inequality (24). There is an intermediate range of density, $0\le\rho_{c_1}\le\rho_m\le\rho_{c_2}$, in which $\bar{V}(\rho_m,\gamma\rho_n)$ is so sensitive to the change in ρ_m that the homogeneous flow is unstable. Following inequality (24), we can find the critical values (ρ_{c_1} and ρ_{c_2}) from the equation

$$(\rho_m^0)^2-\left(\frac{2\beta c_m^0}{\bar{V}_m'}\right)\rho_m^0+\left[\frac{(1+\beta^2)}{2T_m\bar{V}_m'}\right]=0. \quad (25)$$

The speed of the critical disturbances is given by

$$\bar{C}(\rho_m^0)=\bar{V}(\rho_m^0)+\bar{V}'(\rho_m^0)\left(\rho_m^0+\frac{\beta}{2\,T_m c_m^0}\right), \quad (26)$$

which is slower than the steady state traffic speed $v_m^0 = \bar{V}_m(\rho_m^0, \gamma\rho_n^0)$, since $\bar{V}_m'$ is negative. This is in accordance with the kinematic wave speed for a single lane (when $\gamma = 0$) mentioned in Ref. [19]

3. Numerical simulation

In this section, we present the numerical method for the multilane new anisotropic model using the finite difference method. In doing so, the freeway to be modeled is divided into I nodes and the period of analysis into J time steps. The following difference equations are obtained by applying the finite difference scheme on the set of partial differential Eqs. (9) and (10):

$$\begin{aligned}
&\rho_m(i,j+1)\\
&= \rho_m(i,j) + \frac{\Delta t}{\Delta x}\rho_m(i,j)(v_m(i,j) - v_m(i+1,j))\\
&\quad + \frac{\Delta t}{\Delta x}v_m(i,j)(\rho_m(i-1,j) - \rho_m(i,j))\\
&\quad + \Delta t(s_{nm}(i,j) - s_{mn}(i,j)). \qquad (27)
\end{aligned}$$

a) For heavy traffic (i.e., $v_m(i,j) < -2\beta c_m\rho_m(i,j)$)

$$\begin{aligned}
&v_m(i,j+1)\\
&= v_m(i,j) + \frac{\Delta t}{\Delta x}\Big(- 2\beta c\rho_m(i,j) - v_m(i,j)\Big)\\
&\quad \times (v_m(i+1,j) - v_m(i,j))\\
&\quad - \frac{\Delta t}{\tau}(v_m(i,j) - \bar{V}_m)\\
&\quad + \frac{\Delta t}{\tau}\bar{V_m}'\Bigg[\frac{\rho_m(i-1,j) - \rho_m(i,j)}{2\Delta x\rho_m(i,j)}\\
&\quad + \frac{\rho_m(i-1,j) - 2\rho_m(i,j) + \rho_m(i+1,j)}{6(\Delta x)^2(\rho_m(i,j))^2}\\
&\quad - \frac{\rho_m(i-1,j) - \rho_m(i,j)^2}{2(\Delta x)^2(\rho_m(i,j))^3}\Bigg]\\
&\quad + r_1\Delta t s_{nm}(i,j) - r_2\Delta t s_{mn}(i,j); \qquad (28)
\end{aligned}$$

b) for light traffic (i.e., $v_m(i,j) \geq -2\beta c_m\rho_m(i,j)$)

$$\begin{aligned}
&v_m(i,j+1)\\
&= v_m(i,j) + \frac{\Delta t}{\Delta x}\Big(- 2\beta c\rho_m(i,j) - v_m(i,j)\Big)\\
&\quad \times (v_m(i,j) - v_m(i-1,j))\\
&\quad - \frac{\Delta t}{\tau}(v_m(i,j) - \bar{V}_m)\\
&\quad + \frac{\Delta t}{\tau}\bar{V_m}'\Bigg[\frac{\rho_m(i-1,j) - \rho_m(i,j)}{2\Delta x\rho_m(i,j)}\\
&\quad + \frac{\rho_m(i-1,j) - 2\rho_m(i,j) + \rho_m(i+1,j)}{6(\Delta x)^2(\rho_m(i,j))^2}\\
&\quad - \frac{(\rho_m(i-1,j) - \rho_m(i,j))^2}{2(\Delta x)^2(\rho_m(i,j))^3}\Bigg]\\
&\quad + r_1\Delta t s_{nm}(i,j) - r_2\Delta t s_{mn}(i,j), \qquad (29)
\end{aligned}$$

where indexes i and j represent the road section and the time, respectively, and $m, n = 1, 2$. Here Δt and Δx are the grid sizes of the finite difference mesh in time and space dimensions, respectively.

The above difference scheme is suitable for the traffic flow, as it maintains the physical properties of the traffic flow even under extreme conditions. These equations give the density and the velocity at the i-th node of the m-th lane at time step $j+1$ obtained from the known values at the previous time step j.

4. Shock and rarefaction waves

As already pointed out by Daganzo,[9] shock and rarefaction waves are important traffic flow conditions, and the realistic description of the shock fronts in traffic is a particularly difficult problem. Numerical tests are carried out to investigate whether our model can describe the congestion and the dissipation of the traffic flow. Let us consider the two Riemann initial conditions, one describing the congested upstream and nearly free downstream and vice versa on the two lanes. These two conditions are

$$\text{(i)} \quad \begin{cases} \rho_{1\mathrm{u}}^1 = 0.03, \\ \rho_{2\mathrm{u}}^1 = 0.04, \end{cases} \quad \begin{cases} \rho_{1\mathrm{d}}^1 = 0.12, \\ \rho_{2\mathrm{d}}^1 = 0.18, \end{cases} \qquad (30a)$$

$$\text{(ii)} \quad \begin{cases} \rho_{1\mathrm{u}}^2 = 0.12, \\ \rho_{2\mathrm{u}}^2 = 0.18, \end{cases} \quad \begin{cases} \rho_{1\mathrm{d}}^2 = 0.03, \\ \rho_{2\mathrm{d}}^2 = 0.04, \end{cases} \qquad (30b)$$

where $\rho_{1\mathrm{u}}^1$, $\rho_{2\mathrm{u}}^1$, $\rho_{1\mathrm{u}}^2$, $\rho_{2\mathrm{u}}^2$ and $\rho_{1\mathrm{d}}^1$, $\rho_{2\mathrm{d}}^1$, $\rho_{1\mathrm{d}}^2$, $\rho_{2\mathrm{d}}^2$ are, respectively, the upstream and the downstream densities of the two lanes. These situations are realistic in the traffic flow and correspond to a situation where nearly free-flow traffic meets a queue of nearly stopping vehicles, i.e., a shock-wave situation. While the following condition (31) is just opposite to condition (30) and corresponds to a situation of a dissolving queue, i.e., the rarefaction wave situation.

For the initial speed conditions, we take

$$v_{1\mathrm{u}}^{1,2} = \bar{V}_1(\rho_{1\mathrm{u}}^{1,2}, \rho_{2\mathrm{u}}^{1,2}), \quad v_{1\mathrm{d}}^{1,2} = \bar{V}_1(\rho_{1\mathrm{d}}^{1,2}, \rho_{2\mathrm{d}}^{1,2}), \qquad (31a)$$

$$v_{2\mathrm{u}}^{1,2} = \bar{V}_2(\rho_{1\mathrm{u}}^{1,2}, \rho_{2\mathrm{u}}^{1,2}), \quad v_{2\mathrm{d}}^{1,2} = \bar{V}_2(\rho_{1\mathrm{d}}^{1,2}, \rho_{2\mathrm{d}}^{1,2}). \qquad (31b)$$

The equilibrium speed-density relationship developed by Del Castillo and Benitez[31] is modified by substituting $\rho_m + \gamma\rho_n$ and is given as

$$\bar{V}_1(\rho) = v_{1\mathrm{f}}\Bigg[1 - \exp\Bigg(1 - \exp\Bigg(\frac{c_{1,\mathrm{jam}}}{v_{1\mathrm{f}}}$$

$$\times\left(\frac{\rho_{1,\mathrm{jam}}+\gamma\rho_{2,\mathrm{jam}}}{\rho_1+\gamma\rho_2}-1\right)\right)\right)\Bigg], \quad (32a)$$

$$\bar{V}_2(\rho) = v_{2\mathrm{f}}\Bigg[1-\exp\left(1-\exp\left(\frac{c_{2,\mathrm{jam}}}{v_{2\mathrm{f}}}\right.\right.$$
$$\times\left(\frac{\rho_{2,\mathrm{jam}}+\gamma\rho_{1,\mathrm{jam}}}{\rho_2+\gamma\rho_1}-1\right)\right)\right)\Bigg], \quad (32b)$$

where $v_{1,\mathrm{f}}$, $v_{2,\mathrm{f}}$ and $\rho_{1,\mathrm{jam}}$, $\rho_{2,\mathrm{jam}}$ are the free flow speeds and the maximum or the jam densities of lanes 1 and 2, respectively, $c_{1,\mathrm{jam}}$ and $c_{2,\mathrm{jam}}$ are the kinematic wave speeds under jam densities $\rho_{1,\mathrm{jam}}$ and $\rho_{2,\mathrm{jam}}$, respectively. The free boundary conditions are used, i.e., $\partial\rho_m/\partial x$ and $\partial v_m/\partial x$ are equal to zero on both sides.[12,17,27]

We take a test road section of 20 km long. For the numerical calculations, it is divided into 100 meshes of equal length. According to real observation and the parameter identification process, the parameter values are chosen as follows:

$$\begin{aligned}
&v_{1\mathrm{f}} = 40\ \mathrm{m/s}, \quad \rho_{1,\mathrm{jam}} = 0.15\ \mathrm{m}^{-1}, \quad T_1 = 8\ \mathrm{s},\\
&c_{1,\mathrm{jam}} = 7\ \mathrm{m/s}, \quad v_{2\mathrm{f}} = 30\ \mathrm{m/s}, \quad \rho_{2,\mathrm{jam}} = 0.2\ \mathrm{m}^{-1},\\
&T_2 = 7\ \mathrm{s}, \quad c_{2,\mathrm{jam}} = 6\ \mathrm{m/s}, \quad a = 0.01,\\
&b = 5\ \mathrm{s}, \quad \gamma = 0.1, \quad \sigma = \phi = 1, \quad \text{and} \quad \beta = 2. \quad (33)
\end{aligned}$$

Note that the jam density of lane 2 is higher than that of lane 1. Figures 1–6 depict the wave that develops from the Riemann initial conditions (30a) and (30b). Figures 1, 2, 4 and 5 show that different Riemann conditions lead to different fronts between the congested and the free-flow traffics, which results in density changing on both lanes with lane change (Figs. 3 and 6). Figures 1 and 2 show how the backward moving shock-wave front evolves under condition (30a) on lanes 1 and 2, respectively. It shows that the traffic becomes more congested, which is often seen during rush hours. Figures 4 and 5 describe how the rarefaction wave front evolves under condition (30b) on both lanes. It is clear from Figs. 4 and 5 that the moving front is smoothed over time and eventually leads to a continuous traffic flow, which shows the consistency of our model with real traffic flow. There is a queue in the process of dissolution, which is consistent with our daily experiences in real traffic. Such types of results are also found by Han *et al.*[26] and Hua and Han.[27] Figures 3 and 6 show that the lane-changing behaviour occurs more frequently at large densities than that at small densities on both lanes.

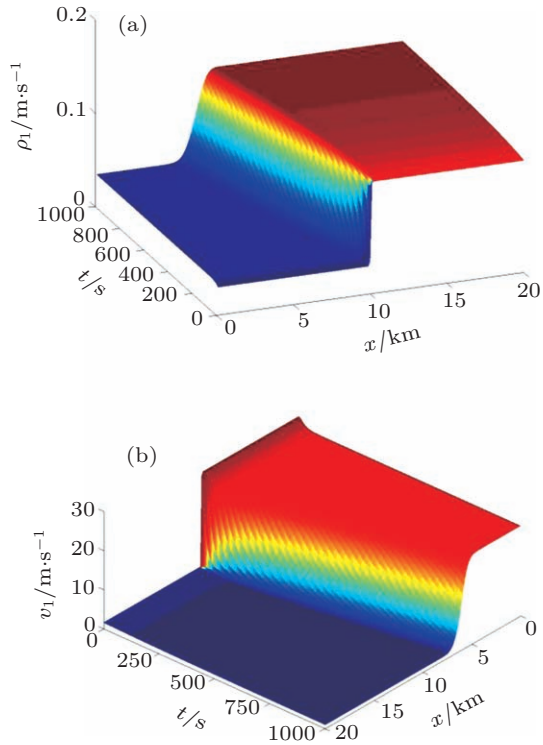

Fig. 1. (colour online) Shock waves under the Riemann initial conditions of Eq. (30a). Panels (a) and (b) show temporal evaluations of density $\rho_1(x,t)$ and velocity $v_1(x,t)$ on lane 1, respectively.

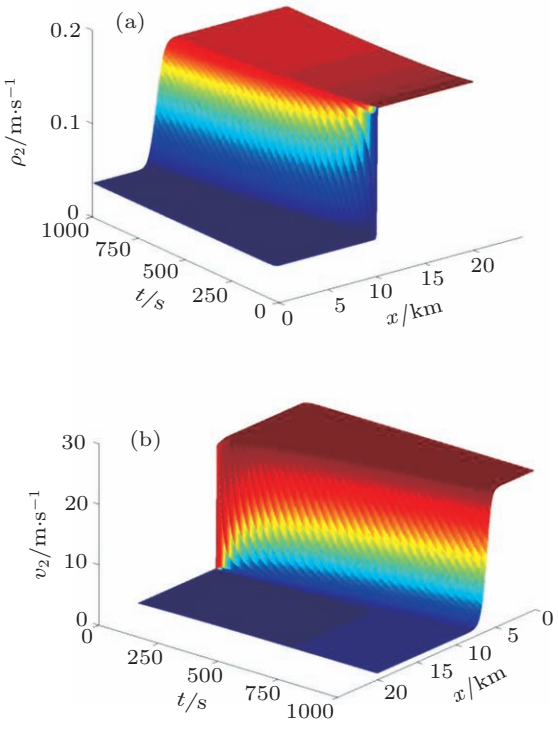

Fig. 2. (colour online) Shock waves under the Riemann initial conditions of Eq. (30a). Panels (a) and (b) show temporal evaluations of density $\rho_2(x,t)$ and velocity $v_2(x,t)$ on lane 2, respectively.

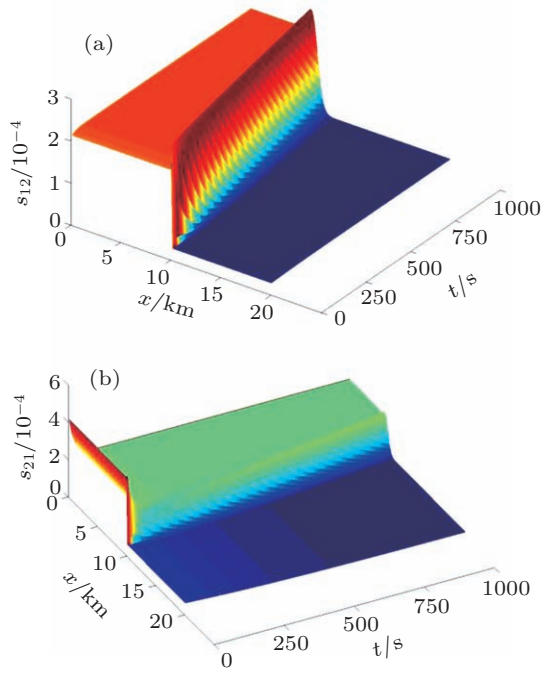

Fig. 3. (colour online) Lane change rates under the Riemann initial conditions of Eq. (30a), where (a) s_{12} is the lane change rate from lane 1 to lane 2, and (b) s_{21} is the lane change rate from lane 2 to lane 1.

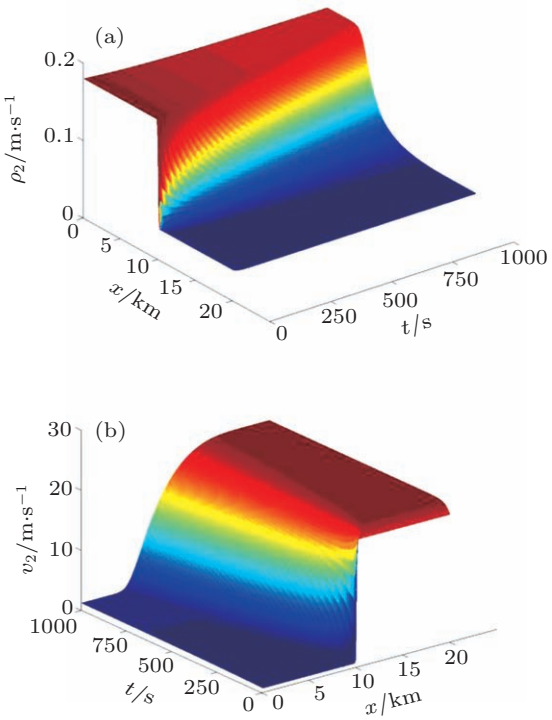

Fig. 5. (colour online) Rarefaction waves under the Riemann initial conditions of Eq. (30b). Panels (a) and (b) show temporal evaluations of density $\rho_2(x,t)$ and velocity $v_2(x,t)$ on lane 2, respectively.

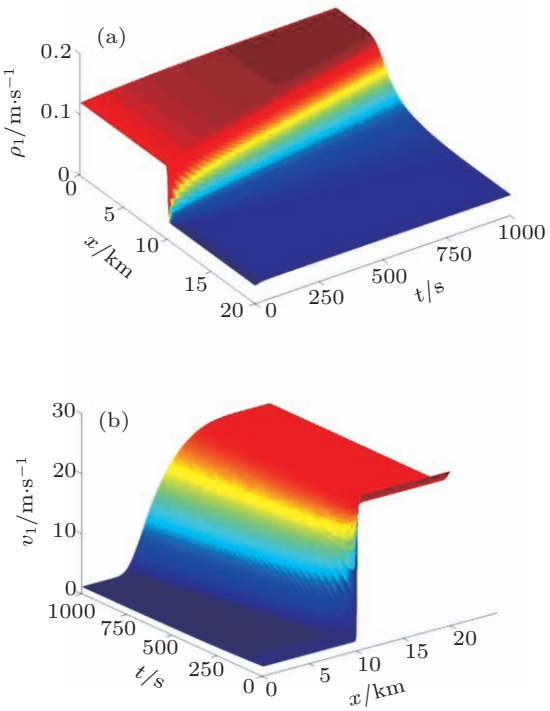

Fig. 4. (colour online) Rarefaction waves under the Riemann initial conditions of Eq. (30b). Panels (a) and (b) show temporal evaluations of density $\rho_1(x,t)$ and velocity $v_1(x,t)$ on lane 1, respectively.

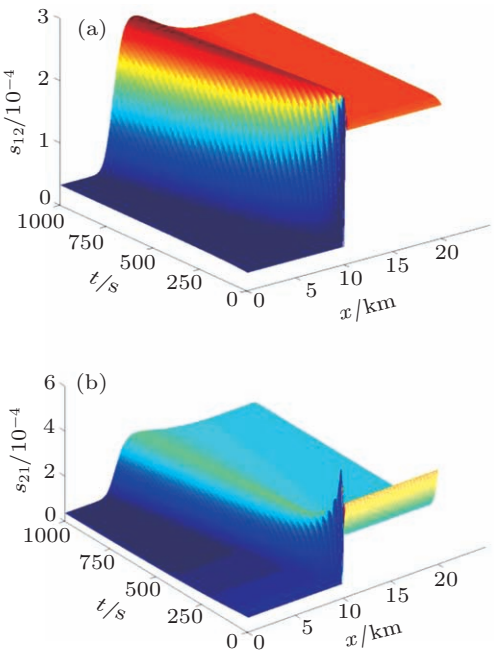

Fig. 6. (colour online) Lane change rate under the Riemann initial conditions of Eq. (30b), where (a) s_{12} is the lane change rate from lane 1 to lane 2, and (b) s_{21} is the lane change rate from lane 2 to lane 1.

5. Local cluster effect

The new multilane model can also describe the nonlinear theory of the cluster effect in a traffic flow, i.e., the effect of the appearance of a region of high density and low average velocity vehicles in an initially homogeneous flow. To investigate the local cluster effect, we apply the numerical scheme given in Section 4. Let us consider the behaviour of a small localized perturbation given by Herrmann and Kerner,[32] which occurs at time $t = 0$ in an initial homogeneous state of traffic flow and is given by

$$\rho_m(x,0) = \rho_{mh} + \Delta\rho_{m0}\left\{\cosh^{-2}\left[\frac{160}{L}\left(x - \frac{5L}{16}\right)\right] - \frac{1}{4}\cosh^{-2}\left[\frac{40}{L}\left(x - \frac{11L}{32}\right)\right]\right\}, \quad (34)$$

$$v_m(x,0) = \bar{V}_m(\rho_m(x,0)), \quad (35)$$

where $x \in [0, L]$, and L is the length of the road section under consideration. The periodic boundary condition to describe the amplification of small disturbances is used and is given by

$$\rho_m(L,t) = \rho_m(0,t), \quad v_m(L,t) = v_m(0,t). \quad (36)$$

For the equilibrium speed-density relationship, the relation proposed by Kerner and Konhäuser[4] is modified by substituting $\rho_m + \gamma\rho_n$ in place of the density and is defined as

$$\bar{V}_m(\rho) = u_{mf}\left\{\left[1 + \exp\left(\frac{(\rho_m + \gamma\rho_n)/\rho_{m,\mathrm{jam}} - 0.25}{0.06}\right)\right]^{-1} - 3.72 \times 10^{-6}\right\}. \quad (37)$$

For the computational purpose, the space domain is divided into equal intervals of length 200 m, and the time interval is chosen to be 1 s.

We take the following set of parameters to show that our model can also describe the local cluster effect of the traffic flow:[17,23,27]

$$\begin{aligned} &v_{1\mathrm{f}} = 40 \text{ m/s}, \quad \rho_{1,\mathrm{jam}} = 0.15 \text{ m}^{-1}, \\ &\Delta\rho_{10} = 0.008 \text{ m}^{-1}, \quad T_1 = 8 \text{ s}, \\ &v_{2\mathrm{f}} = 30 \text{ m/s}, \quad \rho_{2,\mathrm{jam}} = 0.2 \text{ m}^{-1}, \\ &\Delta\rho_{20} = 0.001 \text{ m}^{-1}, \quad T_2 = 7 \text{ s}, \quad a = 0.01, \\ &b = 5 \text{ s}, \quad \gamma = 0.1, \quad \sigma = \phi = 1, \quad \text{and} \quad \beta = 2. \end{aligned} \quad (38)$$

The steady states on both lanes are presented in Fig. 7. At small densities, the flows on both lanes increase with the increase of the density. Note that on the fast lane (first lane), the flow rate reaches the maximum at a smaller density ρ_{c1}, while on the slow lane (second lane), it reaches at ρ_{c2}. In the density range of $\rho_{c1} < \rho < \rho_{c2}$, the flow rate on the first lane decreases, that on the second lane increases, and they become equal at ρ_c. Below ρ_c, the flow on the fast lane is always greater than that on the slow lane. Above ρ_c, the flow on the slow lane become greater than that on the fast lane. This is consistent with the findings of Tang *et al.*[25]

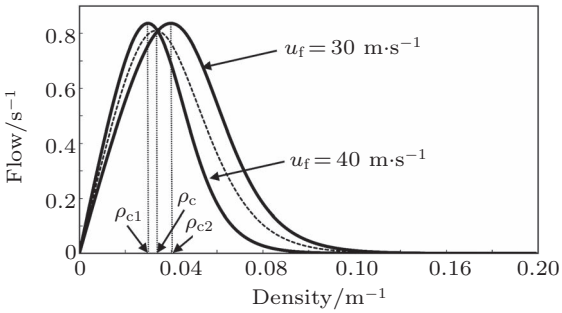

Fig. 7. Fundamental diagram of the steady states of asymmetric two-lane traffic.

To reproduced the lane usage inversion phenomenon, we consider three different cases, in which the initial densities on both lanes are the same and equal to ρ_c, less than ρ_c, and greater than ρ_c, respectively. The three cases are shown graphically in Figs. 8–10, respectively. Figure 8 depicts the spatio–temporal patterns of the density on both lanes when the initial density on each lane is less than ρ_c. It is clear from Figs. 8(a)–8(d) that some vehicles change lanes from lane 2 to lane 1, as below ρ_c, the flow rate on lane 1 is larger than that on lane 2. Figures 9(a)–9(d) show that when the initial densities on both lanes are equal to ρ_c, then there is no lane change except at the location of the perturbation. If $\rho_{mh} > \rho_c$, more vehicles prefer to drive on lane 2 rather than to be trapped on lane 1 (Figs. 10(a)–10(d)). So, ρ_c appears as an inversion point, where the vehicles are evenly distributed on both lanes.

The critical values ρ^*_{c1} and ρ^*_{c2} for lanes 1 and 2 with the parameters given in Eq. (38) are 0.02539 m^{-1}, 0.0714 m^{-1} and 0.0351 m^{-1}, 0.0932 m^1, respectively, which can be found out easily by substituting the parameter values into the stability condition (25). Taking different values of the initial density for the sets of parameters given in Eq. (38), we investigate the traffic density pattern with respect to time, and the results are shown in Figs. 11–15.

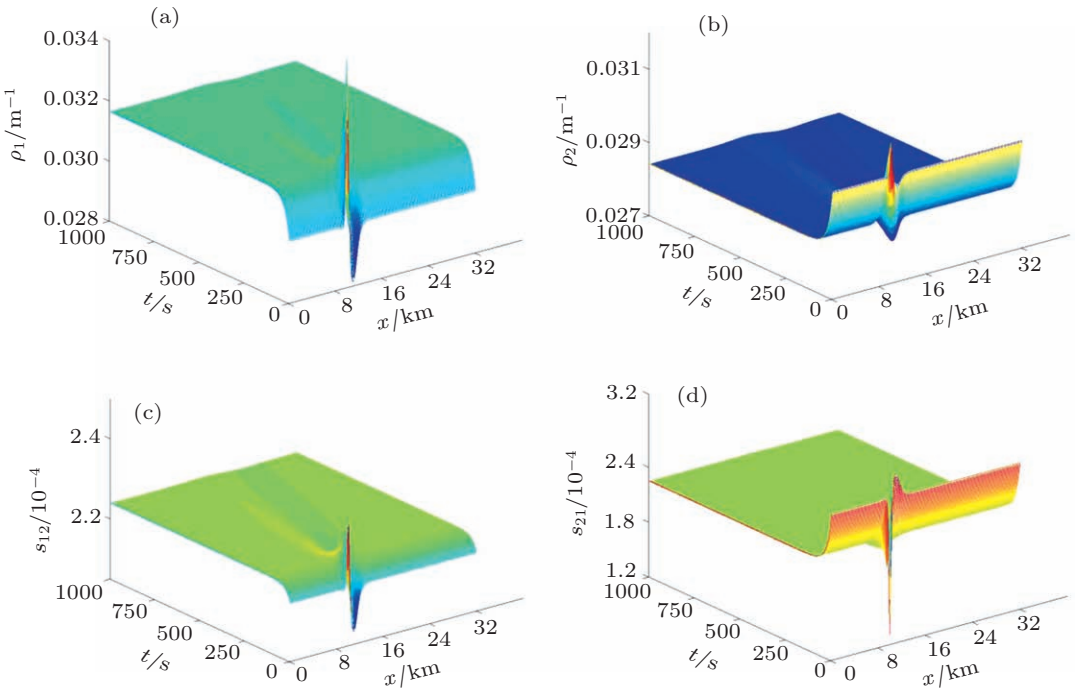

Fig. 8. (colour online) (a) Temporal evolution of traffic density $\rho_1(x,t)$ on lane 1, (b) temporal evolution of traffic density $\rho_2(x,t)$ on lane 2, (c) lane change rate from lane 1 to lane 2 (s_{12}), and (d) generation rate from lane 2 to lane 1 (s_{21}) for $\rho_{1\mathrm{h}} = \rho_{2\mathrm{h}} = 0.03$ m^1 ($< \rho_{\mathrm{c}}$) and $\Delta\rho_0 = 10$ m^{-1}.

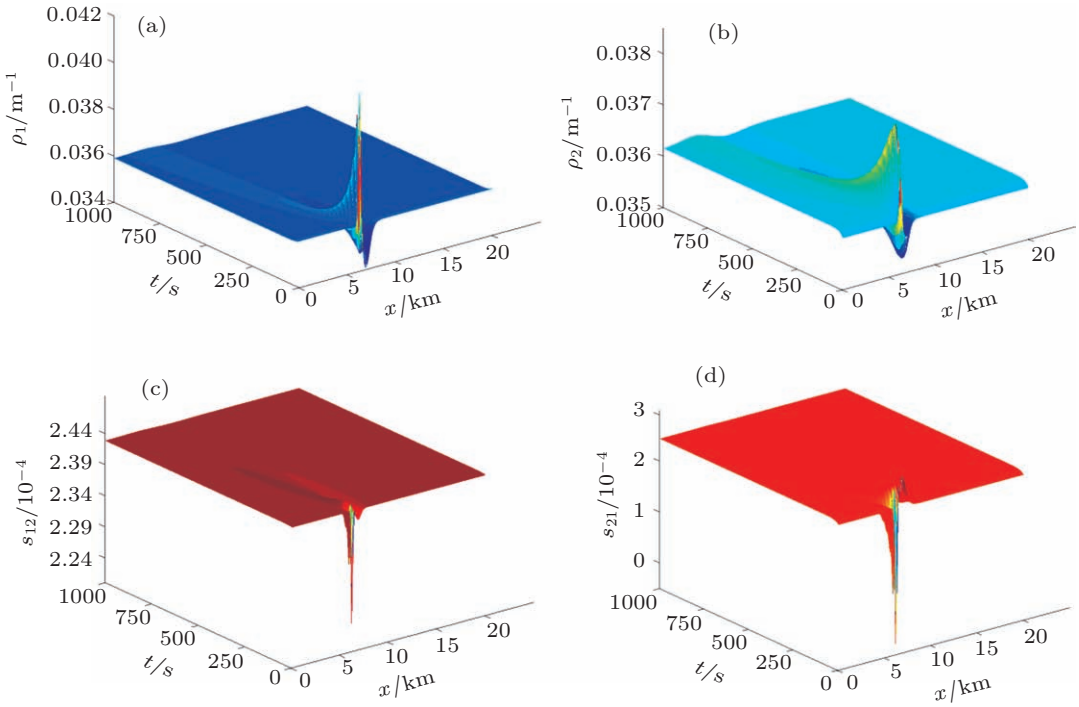

Fig. 9. (colour online) (a) Temporal evolution of traffic density $\rho_1(x,t)$ on lane 1, (b) temporal evolution of traffic density $\rho_2(x,t)$ on lane 2, (c) lane change rate from lane 1 to lane 2 (s_{12}), and (d) generation rate from lane 2 to lane 1 (s_{21}) for $\rho_{1\mathrm{h}} = \rho_{2\mathrm{h}} = \rho_{\mathrm{c}} = 0.035$ m^1 and $\Delta\rho_0 = 0.001$ m^{-1}.

Figure 11 shows that under the uncongested traffic conditions, when the traffic flow density is below the critical density on both lanes, the perturbation dissipates with time and the traffic flows on both lanes are stable. As the traffic density is very low, only a few vehicles change their lanes. Therefore, the front vehicle can speed up freely, which results in the perturbation wave surface propagating in the backward direction. This is

in good agreement with Han *et al.*,[26] Hua and Han,[27] and Herrman and Kerner theories[32] that below the critical density, the initially homogeneous state of the traffic flow is stable with respect to the growth of any non-homogeneous perturbations with small enough amplitudes.

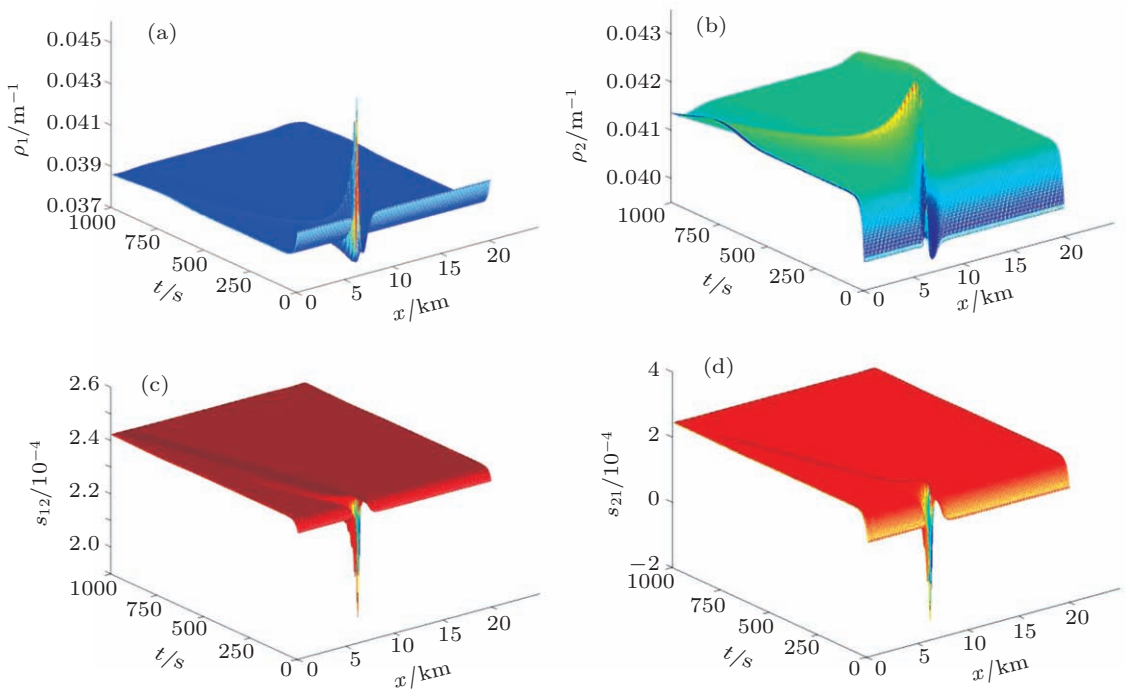

Fig. 10. (colour online) (a) Temporal evolution of traffic density $\rho_1(x,t)$ on lane 1, (b) temporal evolution of traffic density $\rho_2(x,t)$ on lane 2, (c) lane change rate from lane 1 to lane 2 (s_{12}), and (d) generation rate from lane 2 to lane 1 (s_{21}) for $\rho_{1\mathrm{h}} = \rho_{2\mathrm{h}} = 0.04$ m^1 ($> \rho_\mathrm{c}$) and $\Delta\rho_0 = 0.001$ m^{-1}.

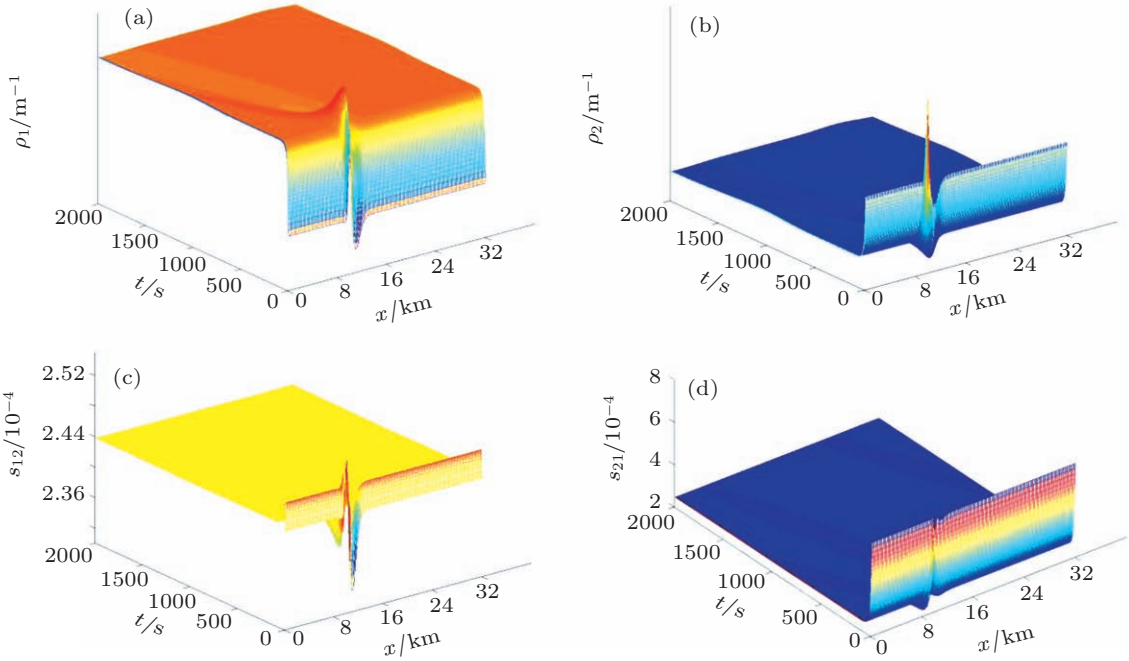

Fig. 11. (colour online) (a) Temporal evolution of traffic density $\rho_1(x,t)$ on lane 1, (b) temporal evolution of traffic density $\rho_2(x,t)$ on lane 2, (c) lane change rate from lane 1 to lane 2 (s_{12}), and (d) generation rate from lane 2 to lane 1 (s_{21}) for $\rho_{1\mathrm{h}} = 0.031$ m^{-1} and $\rho_{2\mathrm{h}} = 0.045$ m^{-1}.

When the traffic density on lane 2 is increased to a certain level while the density on lane 1 remains unchanged, a traffic breakdown may occur if the perturbation is exerted to both lanes. Figure 12 shows that when the initial density is just above the down critical density, a single local cluster forms on both lanes and moves in the backward direction. In this situation, a number of vehicles on both lanes change their lanes, which can be seen in Figs. 12(c) and 12(d). This leads to the conclusion that a higher frequency of lane changing occurs at large densities, which is consistent with our daily experiences and the results obtained by Hua and Han.[27]

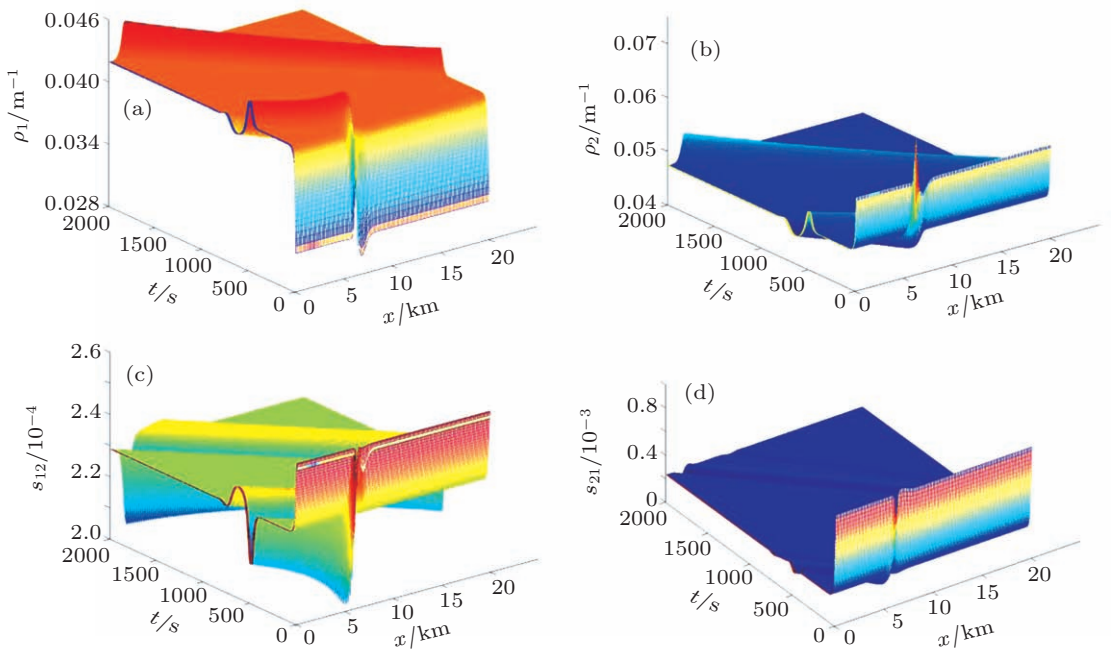

Fig. 12. (colour online) (a) Temporal evolution of traffic density $\rho_1(x,t)$ on lane 1, (b) temporal evolution of traffic density $\rho_2(x,t)$ on lane 2, (c) lane change rate from lane 1 to lane 2 (s_{12}), and (d) generation rate from lane 2 to lane 1 (s_{21}) for $\rho_{1\mathrm{h}} = 0.031$ m^{-1} and $\rho_{2\mathrm{h}} = 0.058$ m^{-1}.

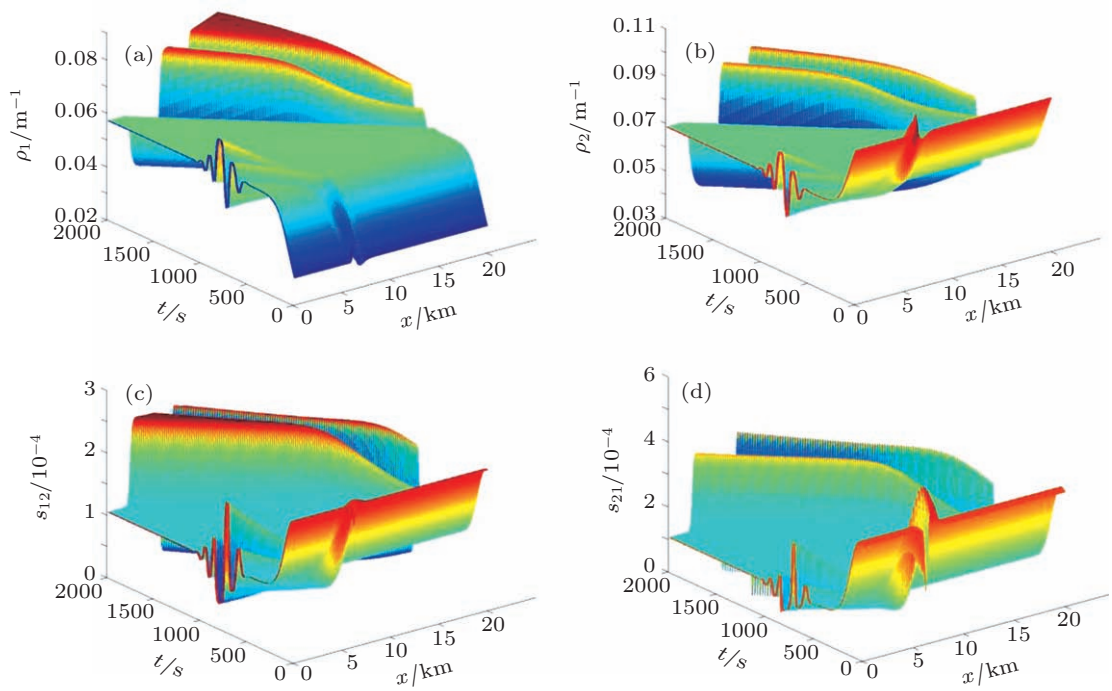

Fig. 13. (colour online) (a) Temporal evolution of traffic density $\rho_1(x,t)$ on lane 1, (b) temporal evolution of traffic density $\rho_2(x,t)$ on lane 2, (c) lane change rate from lane 1 to lane 2 (s_{12}), and (d) generation rate from lane 2 to lane 1 (s_{21}) for $\rho_{1\mathrm{h}} = 0.031$ m^{-1} and $\rho_{2\mathrm{h}} = 0.095$ m^{-1}.

Further increasing the initial density of lane 2 to 0.095 while keeping that of lane 1 fixed at 0.031 leads to a complex localized structure of two or more clusters, as illustrated in Fig. 13. The situation of the multiple clusters corresponds to a stop-and-go traffic. Figures 13(c) and 13(d) show that lane 1 attracts a considerable number of vehicles from lane 2.

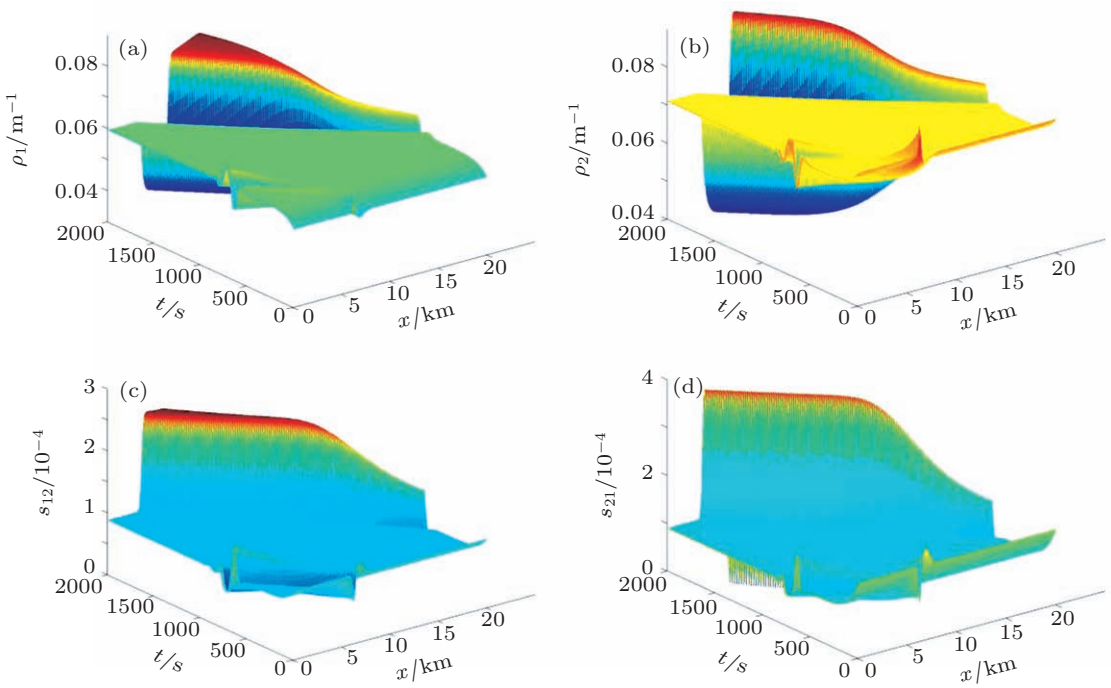

Fig. 14. (colour online) (a) Temporal evolution of traffic density $\rho_1(x,t)$ on lane 1, (b) temporal evolution of traffic density $\rho_2(x,t)$ on lane 2, (c) lane change rate from lane 1 to lane 2 (s_{12}), and (d) generation rate from lane 2 to lane 1 (s_{21}) for $\rho_{1\mathrm{h}} = 0.055\ \mathrm{m}^{-1}$ and $\rho_{2\mathrm{h}} = 0.045\ \mathrm{m}^{-1}$.

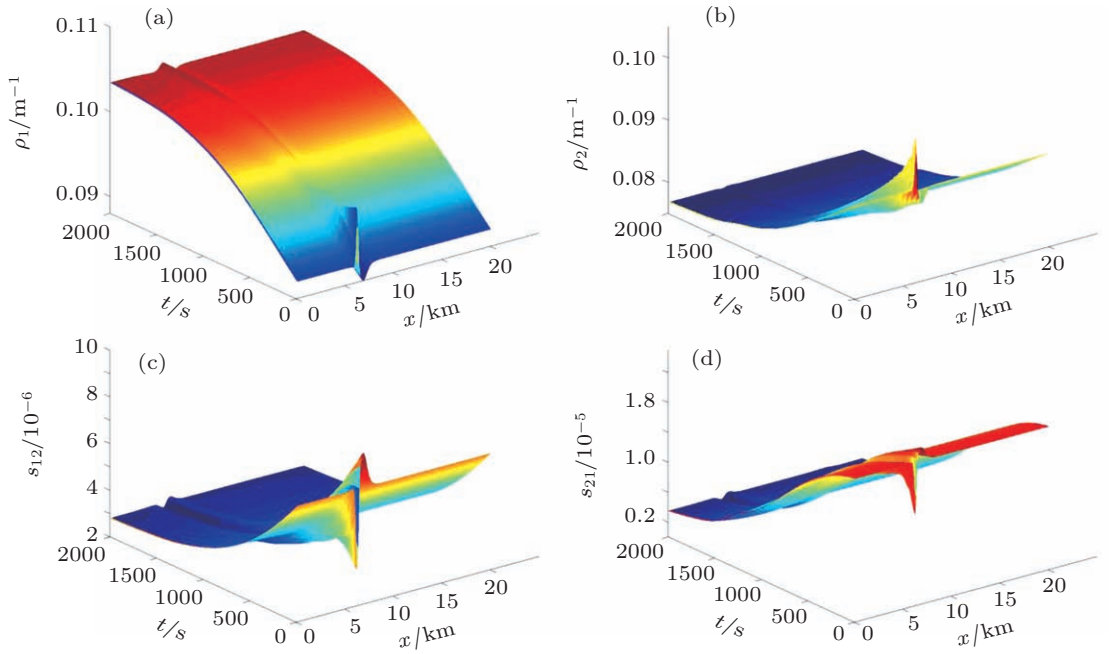

Fig. 15. (colour online) (a) Temporal evolution of traffic density $\rho_1(x,t)$ on lane 1, (b) temporal evolution of traffic density $\rho_2(x,t)$ on lane 2, (c) lane change rate from lane 1 to lane 2 (s_{12}), and (d) generation rate from lane 2 to lane 1 (s_{21}) for $\rho_{1\mathrm{h}} = 0.09\ \mathrm{m}^{-1}$, $\rho_{2\mathrm{h}} = 0.09\ \mathrm{m}^{-1}$.

When the density on lane 1 is increased to 0.055 while the density on lane 2 remains 0.095, a dipole-like structure on both lanes is obtained, as illustrated in Fig. 14. Figures 14(c) and 14(d) show that even in the dipole-like situation, lane-changing occurs. Finally, it is clear from Fig. 15 that as the densities on both lanes become greater than the up-critical density, a stable regime is reached again on both lanes. Lane-changing hardly occurs in this situation, as shown in Figs. 15(c) and 15(d).

The above results show good agreement with the results found by Huang *et al.*,[23] Hua and Han,[27] and Herrmann and Kerner.[32]

6. Conclusion

In the literature of the macroscopic traffic theory, especially that of higher-order models, research on shock and rarefaction waves and the cluster effect are important. Many previously developed higher-order models mainly describe single lane traffic while leaving multilane problems insufficiently discussed. In this paper, we present a multilane generalization of a new anisotropic continuum traffic flow model. A new single lane traffic flow model is derived from the car-following model and practically includes some of the well-known non-equilibrium models as special cases. However, an important difference between the new and the previously developed models is that our model can be isotropic. The isotropic behaviour can be controlled by an anisotropic factor β. In the limit of $\beta \to \infty$, the isotropic behaviour dies out and the model becomes fully anisotropic.

Lane-changing behaviour is incorporated into the extended GK model by introducing a source term and a sink term of lane-changing rate, the coupling effect between two lanes in the continuity equation, and two corresponding terms in the speed dynamic equations. Due to the separately modelings of the source term, the sink term, and the coupling effect, the lane changing rate may be investigated in our model.

The conditions for securing the linear stability of the new model are presented. The shock and the rarefaction waves together with the vehicle clustering are investigated numerically in the extended two-lane GK model. We present a simple finite difference scheme to carry out the numerical simulation and discuss the applicability of the scheme in some special cases. Finally, the numerical tests verify that the multilane continuum model is able to describe the vehicle movement and the amplification of small perturbations, and reproduce some complex nonequilibrium traffic phenomena, such as the stop-and-go, the ghost jams, the local cluster, and the phase transition.

The findings obtained in this study reveal that the two-lane continuum model is much more complicated than that of the single lane traffic due to the existence of the lane-changing. The lane-changingmay improve the traffic in some cases; however, it may worsen the situation in some other cases. Further investigations need to be carried out to test the performance of the new anisotropic continuum model in modelling real traffic. So it may be reasonable to conclude that the new multi-lane model provides a more accurate description of the traffic flow and the results obtained are consistent with the spectrum of the nonlinear dynamic properties reported in the literature.

References

[1] Lighthill M J and Whitham G B 1955 *Proc. Roy. Soc. Lond. Ser.* A **229** 317
[2] Helbing D 1996 *Phys. Rev.* E **53** 2366
[3] Payne H J 1971 *Simulation Councils Proc. Ser.* **1** 51
[4] Kerner B S and Konhäuser P 1993 *Phys. Rev.* E **48** 2335
[5] Zhang H M 1998 *Trans. Res.* B **32** 485
[6] Berg P, Mason A and Woods A 2000 *Phys. Rev.* E **61** 1056
[7] Richards P I 1956 *Operations Research* **4** 42
[8] Bando M, Hasebe K, Nakayama A, Shibata A and Sugiyama Y 1995 *Phys. Rev.* E **51** 1035
[9] Daganzo C F 1995 *Trans. Res.* B **29** 277
[10] Zhang H M 2000 *Trans. Res.* B **34** 583
[11] Aw A and Rascle M 2000 *SIAM J. Appl. Math.* **60** 916
[12] Jiang R, Wu Q S and Zhu Z 2002 *Trans. Res.* B **36** 405
[13] Zhang H M 2002 *Trans. Res.* B **36** 275
[14] Jiang R and Wu Q S 2004 *Acta Mech. Sin.* **20** 106
[15] Jiang R and Wu Q S 2003 *Trans. Res.* B **37** 85
[16] Zhang H M 2003 *Trans. Res.* B **37** 27
[17] Xue Y and Dai S 2003 *Phys. Rev.* E **68** 066123
[18] Gupta A K and Katiyar V K 2005 *J. Phys.* A **38** 4069
[19] Gupta A K and Katiyar V K 2006 *Physica* A **368** 551
[20] Daganzo C F 1997 *Trans. Res.* B **31** 83
[21] Wu Z 1994 *Acta Mech. Sin.* **26** 149
[22] Tang T Q and Huang H J 2004 *Chin. Sci. Bull.* **49** 2097
[23] Huang H J, Tang T Q and Gao Z Y 2006 *Acta Mech. Sin.* **22** 131
[24] Tang T Q and Huang H J 2005 *J. Beijing Univ. Aero. Astro.* **31** 1121
[25] Tang C F, Jiang R and Wu Q S 2007 *Chin. Phys.* **16** 1570
[26] Han P G, Hua S D and Pan H H 2009 *Chin. Phys.* B **18** 468
[27] Hua S D and Han P G 2009 *Chin. Phys.* B **18** 3724
[28] Zhang H M 2003 *Trans. Res.* B **37** 561
[29] Zhou X, Liu Z and Luo J 2002 *J. Phys.* A: *Math. Gen.* **35** 4495
[30] Liu G Q, Lyrintzis A S and Michalopoulos P G 1996 *Appl. Math. Model.* **20** 459
[31] Del Castillo J M and Benitez F G 1995 *Trans. Res.* B **29** 373
[32] Herrmann M and Kerner B S 1998 *Physica* A **255** 163